The Astrophysical Journal, 786:124 (7pp), 2014 May 10 doi:10.1088/0004-637X/786/2/124

THE ORIGIN OF THE SPECTRAL INTENSITIES OF COSMIC-RAY POSITRONS

R. Cowsik[1], B. Burch[1], and T. Madziwa-Nussinov[1]
Physics Department and McDonnell Center for the Space Sciences, Washington University, St. Louis, MO 63130, USA; cowsik@physics.wustl.edu
Received 2013 September 27; accepted 2014 March 17; published 2014 April 24

ABSTRACT

We present a straightforward model of cosmic-ray propagation in the Galaxy that can account for the observed cosmic-ray positrons entirely as secondary products of cosmic-ray interactions with the interstellar medium. In addition to accounting for the observed energy dependence of the ratio of positrons to total electrons, this model can accommodate both the observed energy dependence of secondary to primary nuclei, like boron/carbon, and the observed bounds on the anisotropy of cosmic rays. This model also predicts the energy dependence of the positron fraction at energies higher than those measured to date, with the ratio rising to ∼0.7 at very high energies. The model presented in this paper arises as a natural extension of the widely used current models and allows one to include the spatial and temporal discreteness of the sources of cosmic rays.

Key words: acceleration of particles – astroparticle physics – cosmic rays

Online-only material: color figures

1. INTRODUCTION AND OVERVIEW

The recent measurement of the positron fraction $R_{e+}(E) = F_{e+}/(F_{e+} + F_{e-})$ at energies E up to 300 GeV by the Alpha Magnetic Spectrometer (AMS) collaboration (Aguilar et al. 2013) is an important contribution to cosmic-ray physics and poses a challenge to predict $F_{e+}(E)$ with similar precision. A striking feature of the AMS data, confirming with unprecedented accuracy the earlier observations (Adriani et al. 2009, 2010; Ackerman et al. 2012a), is the monotonic *increase* of $R_{e+}(E)$ from ∼0.052 at ∼10 GeV to ∼0.155 at ∼300 GeV. This observed ratio differs significantly from theoretical predictions of a monotonic *decrease* by current models of cosmic-ray propagation such as that by Moskalenko & Strong (1998, hereafter MS). The observed and theoretically calculated ratios are displayed in the lower panel in Figure 1. This disagreement with the current models has prompted suggestions that the positron excess could either originate from pulsars' magnetospheres (Yuksel et al. 2012; Profumo 2012) or from the annihilation or decay of dark matter (Bergström et al. 2009), an explanation which is constrained by the absence of high energy gamma rays from the center of the Galaxy (Ackerman et al. 2012b). A kinematical cut-off below the dark-matter mass, $M(x)$, at $E \sim ((1/2)-(1/4))M(x)$, in the positron spectrum is viewed by some as an indication of dark matter (Bergström et al. 2013). A similar cut-off is also expected in the pulsar models.

By extending the current models of cosmic-ray propagation to include the discrete nature of the cosmic-ray sources, we show here that the observed decrease of the positron fraction, $R_{e+}(E)$, up to ∼6 GeV and its subsequent increase at higher energies can be explained by treating positrons as just cosmic-ray secondaries. Furthermore our calculations (shown in the lower panel of Figure 1) predict a dip in the positron fraction beyond 300 GeV followed by an increase beyond 1000 GeV to reach an asymptotic value of ∼0.7. A broad set of discussions pertaining to the positron fraction in alternate scenarios may be found in the papers by Blasi (2009), Mertsch & Sarkar (2009), Shaviv et al. (2009) and Katz et al. (2010). Even at the outset, we would like to draw attention to the paper by Cholis & Hooper (2013) who have considered these suggestions that positrons accelerated along with other particles in nearby supernova remnants account for the enhanced positron fraction observed by PAMELA and AMS instruments; Cholis and Hooper, based on the observed B/C ratios, place a strict upper bound of 25% on any such contributions. The comments by Cowsik (1980) and Gaggero et al. (2013) are also relevant in this context. In the Nested Leaky-box (NLB) scenario considered here, the particles are accelerated in a large number of sources sprinkled across the Galaxy. Each of these sources is surrounded by a cocoon-like region where some spallation of the nuclei takes place, but without any reacceleration. Accordingly, such an upper bound derived by Cholis and Hooper is not relevant to the secondary to primary ratios calculated in the model presented in this paper, and this model indeed reproduces correctly the observed abundance ratios of secondary cosmic-ray nuclei, like B/C and ^{10}Be/^{9}Be. This paper is devoted to the presentation of several aspects of this model.

We now review the current models of cosmic-ray propagation, including the MS model and point out specifically how we have modified them to explain the positron fraction observed in the cosmic rays. The current models (Moskalenko & Strong 1998; Strong et al. 2007; Davis et al. 2000) envisage a spatially smooth and temporally constant distribution of sources that inject cosmic rays into the interstellar medium. Subsequently, the cosmic rays are assumed to diffuse through the Galaxy, with a diffusion constant, κ, that increases with energy as $\sim E^{\alpha}$. The secondary nuclei, generated through the spallation of the primary cosmic rays in collisions with the interstellar medium, also propagate with a similar diffusion constant. As cosmic rays reach a height of ∼500 pc above the plane, they leak out and are lost from the Galaxy. Their mean residence time in the Galactic volume, τ, is thus a decreasing function of energy, $\tau \sim 1/\kappa \sim E^{-\alpha}$, indicating rapid leakage of more energetic particles from the Galaxy. Accordingly, in these models, even though at production the spectrum of secondary nuclei is the same as their parent primary nuclei, their steady-state spectra are steeper $\sim E^{-\beta-\alpha}$ and the ratio like B/C is a decreasing function of energy, proportional to $1/\kappa(E)$ or $\tau(E)$, in the leading order. Some current models (Davis et al. 2000), often referred to as the Leaky-box (LB) models, start directly with $\tau(E)$, along with

[1] Campus Box 1105, 1 Brookings Drive, St. Louis, MO 63130, USA.

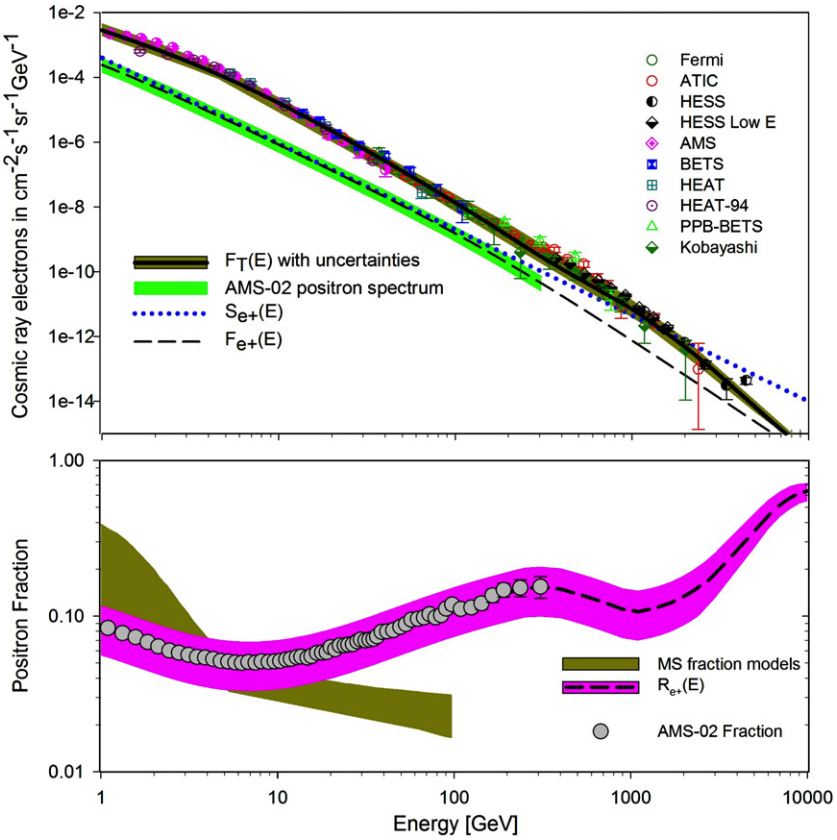

Figure 1. Upper panel: the solid black line represents our fit, $F_T(E)$, to the spectrum of the total electronic component observed in cosmic rays; the band enveloping the dashed and dotted lines show the observed positron spectrum $F_{\rm AMS}$ obtained by multiplying the positron fraction by $F_T(E)$. The dashed line represents the theoretical spectrum, $F_{e+}(E)$, given in Equation (12) and the dotted line represents the spectral shape of positrons at production. Lower panel: our predicted positron fraction, $R_{e+}(E) = F_{e+}(E)/F_T(E)$, with uncertainties is shown; the shaded steeply falling region is due to the MS model.

(A color version of this figure is available in the online journal.)

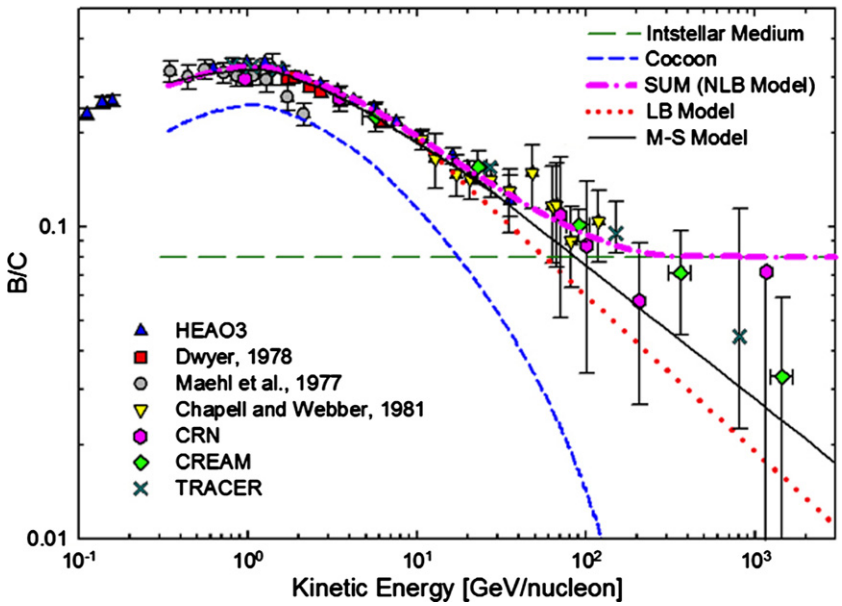

Figure 2. Observed B/C ratio is plotted along with the spectra expected from the MS model and the Nested Leaky-box model (Cowsik & Burch 2010).

(A color version of this figure is available in the online journal.)

an exponential path length distribution (Cowsik et al. 1967) and obtain a good fit to the ratios of secondary to primary nuclei like B/C, which has been observed with good statistics up to ~50 GeV and with decreasing precision at higher energies (see Figure 2). The value of $\alpha \approx 0.6$ has been chosen empirically in Galprop and other current models (Moskalenko & Strong 1998; Davis et al. 2000) to fit the observed ratios like B/C in cosmic rays. Similarly, the positrons are generated in the interstellar

medium mainly through interaction of cosmic-ray protons, and at production have the same spectrum, $\sim E^{-\beta}$. At low energies, where the radiative loss of energy by the positrons is small and their spectrum in steady state, being proportional to τ, also becomes $\sim E^{-\beta-\alpha}$, contrary to the observed spectrum $\sim E^{-\beta}$ up to ~100 GeV. This close correlation between the spectrum of the boron nuclei and of the positrons is inescapable in the context of the current models.

Is there any modification of the current models that will allow us to reconcile them with the different spectral shapes of the observed spectra of boron and the positrons? By noting that the positrons carry away only a small fraction ~3%–5% of the energy of their parent primary cosmic-ray proton, in contrast to ~100% of the energy per nucleon of their parent nuclei by boron, we show in this paper that it is indeed possible to modify the current models to bring them into agreement with all cosmic-ray observations: in the current models, the cosmic-ray sources are treated as spatially smooth and temporally constant; the modification we suggest is to bring in the discrete nature of these sources.

We attribute the falling energy-dependent part of the B/C ratio to the production of boron nuclei through spallation of primary cosmic rays in a cocoon-like region (see Figure 2). There exists both observational and theoretical analysis in support of such regions surrounding regions where energetic particles are accelerated in the Galaxy. For example the *Fermi*-Large Area Telescope has observed a cocoon of freshly accelerated cosmic rays interacting with dense gas generating high energy gamma rays (Ackerman et al. 2011; Binns 2011). In the context of the discussion of supernova shocks, which are one of the promising regions of cosmic-ray acceleration, the evidence for high density circumstellar gas surrounding the supernovae has been reviewed extensively by Chevalier and Fransson before presenting a detailed analysis of the propagation of shocks across such regions (Chevalier & Fransson 2003). The transport of cosmic rays through these circumstellar regions is more rapid at higher energies as evidenced both through theoretical studies and empirical analysis (Telezhinsky et al. 2012; Potgieter 2013). Keeping in mind that boron nuclei are produced in spallation reactions with the same energy per nucleon as their parent nuclei, such as carbon, significant production of secondary nuclei like boron produced in the cocoon-like regions with a relatively steep spectrum, as higher energy parents leak away faster from the cocoon. This is to be contrasted with the production of positrons in these regions: in the production process, positrons carry away only a small fraction 0.03–0.05 of the energy per nucleon of their parent nucleons. Accordingly the generation of even a few GeV positrons requires nucleons of energy ~100 GeV or higher, which get transported away rapidly from the cocoon before suffering significant nuclear interactions (see Figures 2 and 3). Accordingly, the energetic positrons are mostly generated in the interstellar medium, from which cosmic rays are assumed to leak out in an energy-independent fashion, up to a PeV.

2. DESCRIPTION AND ANALYSIS OF OUR MODEL

The spectral intensities of cosmic-ray positrons provide a hitherto unavailable probe for the study of the origins and propagation of cosmic rays. First, positrons are not ubiquitous like electrons that may be accelerated to cosmic-ray energies in the sources; on the other hand, positrons have to be generated as secondaries through the $\pi^+ \rightarrow \mu^+ \rightarrow e^+$ and decay chains of other mesons produced in the cosmic-ray interactions in the interstellar medium. Secondly, in high energy cosmic-ray

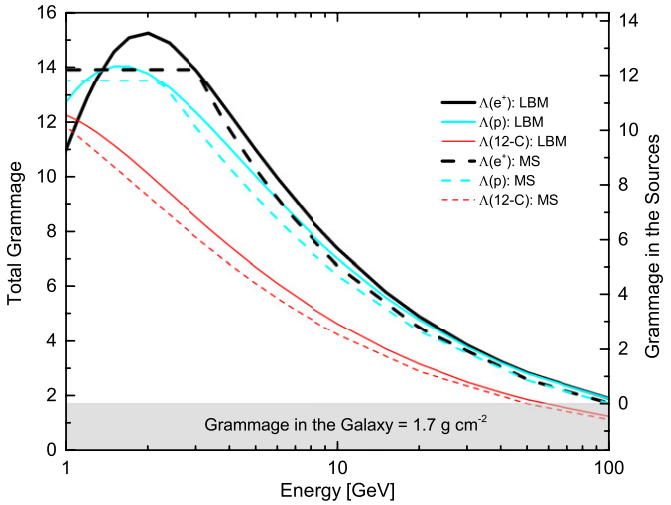

Figure 3. Grammage $\Lambda(E)$ for the various cosmic-ray particles as a function of the kinetic energy per nucleon or per positron is displayed for the Leaky-box model of Davis et al. (Davis et al. 2000) as dashed lines and estimated from the diffusion model of MS (Moskalenko & Strong 1998) as solid lines. In our NLB model, much of the energy dependent part of the grammage is attributed to traversal in the sources and a constant value ~1.7 g cm^{-2}, independent of energy, is traversed in the interstellar medium of the Galaxy.

(A color version of this figure is available in the online journal.)

proton interactions, the positrons carry away only a small fraction ~3%–5% of the energy of the primary nucleon, and the observed spectrum of positrons will carry a signature of its origins. With this is mind, we have calculated the spectrum of positrons, $F_{e+}(E)$, by multiplying the positron fraction measured by the AMS instrument, $R_{e+}(E)$, by $F_T(E)$, a fit to the observed spectrum of the total electronic component, which is very well established. Both these spectra, $F_T(E)$ and $F_{e+}(E)$, are displayed in Figure 1. The PAMELA results (Adriani et al. 2009) are consistent with the compilation of $F_{e+}(E)$ observations displayed here. In the energy interval 3 GeV $\leqslant E <$ 100 GeV, the spectrum of positrons $F_{e+}(E)$ has the form $AE^{-\beta_+}$ with $\beta_+ \sim 2.65$, almost identical with that of the total nuclear component of primary cosmic rays. In contrast, the total electronic component has a spectrum that has a spectral index $\beta_T \approx 2.2$ below a few GeV, steepening to an index of $\beta_T \approx 3.1$ until ~1000 GeV, beyond which there is a rapid decrease of the intensities.

The rate of generation of positrons is well established and, based on the calculations of MS, we estimate the source spectrum of the positrons to be

$$q(E) = q_0 E^{-\beta}, \tag{1}$$

where E is in GeV throughout this paper, $q_0 \approx 5 \times 10^{-27}$ GeV^{-1} s^{-1} (H$_{\rm atom}$)$^{-1}$ and β is the spectral index of the cosmic rays. A recent compilation of cosmic-ray proton and He spectra at high energies (Bernard et al. 2012), yields a spectrum for the nucleons with spectral index ~2.65 in the relevant energy region. In order to obtain the steady state spectrum of positrons, we should account for the energy loss suffered by the positrons through synchrotron radiation and inverse Compton scattering against the 2.7 K microwave background in the Galaxy. The radiation loss is assumed to be smooth and is parameterized as

$$\frac{dE}{dt} = -bE^2, \tag{2}$$

where $b \approx 1.6 \times 10^{-3}\,\mathrm{GeV}^{-1}\,\mathrm{Myr}^{-1}$ (Cowsik & Burch 2010). We note, parenthetically, that the interstellar energy density of starlight is ~0.5 eV cm^{-3} (Cox 1999) and peaks around 400–500 nm corresponding to a mean energy of ~2–2.5 eV per photon (Witt & Johnson 1973). Accordingly, the number density of photons is ~0.2 cm^{-3} and the Thomson scattering mean time becomes ~8 Myr. Thus the energy loss suffered by cosmic-ray electrons through scattering will have a highly stochastic nature. Furthermore, when the energy of the starlight photons in the rest frame of the electrons and positrons approach and exceed $m_e c^2 \sim 0.5$ MeV, the scattering cross sections become smaller compared with the Thomson value and are well represented by the Klein–Nishina formula (Jauch & Rohrlich 1996). Thus at $E \gtrsim 50$ GeV the scattering on starlight photons becomes progressively negligible. At lower energies, since the radiation losses scale as E^2, they have only a marginal effect during the few million years' residence time of cosmic-ray electrons, positrons and other particles in the Galaxy that are needed to generate all the secondaries in our model. The precise value of the parameter b is not needed for an understanding of the general features of the model, as we will see below.

The transport of cosmic-ray positrons and electrons may be described by the equation which includes the spatial diffusion, radiative energy losses and the ultimate leakage from the Galaxy characterized by an effective time τ (Syrovat-skii 1959):

$$\frac{\partial F}{\partial t} - \nabla(\kappa \nabla F) - \frac{d}{dE}(bE^2 F) - \frac{F}{\tau} = Q, \tag{3}$$

where $Q = q(E_0) n_{\rm H}(\boldsymbol{r}) c/4\pi$ represents the source term and $n_{\rm H}$ is the number density of hydrogen in the interstellar medium. It can be shown that the transport equation admits the Green's function

$$G(E, t, \boldsymbol{r}, E_0) = (4\pi\kappa t)^{-3/2} \exp\left(-\frac{r^2}{4\kappa t} - \frac{t}{\tau}\right) \times (1 - bEt)^{-2} \delta\left(E_0 - \frac{E}{1 - bEt}\right). \tag{4}$$

This represents the intensity of electrons or positrons seen at $\boldsymbol{r} = 0$, with energy E, and time t after an impulse of cosmic rays generated by a source at $t = 0$, position $\boldsymbol{r}$, and energy E_0. This Green's function may also be used to analyze the observed spectrum of electrons $F_{e^-}(E)$ due to the sources located at $\boldsymbol{r}_i$ and generating electrons continuously with a power law spectrum $A_i E_0^{-\beta}$

$$F_{e^-}(E) = \sum_i^N \int_0^{1/bE} \int_0^\infty G(E, t, \boldsymbol{r}_i, E_0) A_i E_0^{-\beta} dt dE_0$$

$$= \sum_i^N \int_0^{1/bE} \frac{A_i}{E^\beta} \frac{(1 - bEt)^{\beta-2}}{(4\pi\kappa t)^{3/2}} \exp\left(-r_i^2/4\kappa t\right) \times \exp(-t/\tau) dt \tag{5}$$

noting that in the argument of the delta-function, as $E_0 \to \infty$, $t = 1/bE$, leads to the displayed upper limit on t in Equation (5). At the highest energies $t_{\rm max} = 1/bE$ is small and the dominant contribution to the observed spectrum of electrons is provided by the term $\exp(-r_n^2/4\kappa t)$, with r_n being the distance to the nearest source. Accordingly, the spectrum at the highest energies will be

$$F_{e^-}(E) \sim \exp\left(-r_n^2 bE/4\kappa\right) \sim \exp(-E/E_n). \tag{6}$$

For $r_n = 300$ pc, a rapid steepening of the spectrum of primary electrons is therefore expected at $E_n = 4\kappa/br_n^2 \approx 800$ GeV.

For positrons produced as secondaries in the interstellar medium, the source function, $Q = q_0(E_0) n_{\rm H}(\boldsymbol{r}) c/4\pi$ is continuous, uniform, and is a power-law in energy. The observed spectrum is an integral of the Green's function over these distributions. The distribution $n_{\rm H}$ is well measured over the Galaxy and we approximate this as of uniform density $\bar{n}_{\rm H}$ which extends up to a height $Z_0 \approx 200$ pc above and below the Galactic plane. The radial fall-off in the hydrogen density has a scale length of ~3 kpc, much larger than Z_0. Accordingly, with adequate accuracy, the limits of integration for the radial distance, R, in the plane may be kept as 0 to ∞. The upper limit of the integration over E_0, the maximum energy of the positron at production by the cosmic rays maybe taken to be ∞.

$$F_{e^+\rm ISM}(E) = \frac{c}{4\pi} \int_0^{t_{\rm max}} dt \int_{-Z_0}^{Z_0} dz \int_0^\infty 2\pi R dR \int_0^\infty (4\pi\kappa t)^{-3/2} \times \exp[-(r^2/4\kappa t) - t/\tau]\left(\bar{n}_{\rm H} q_0 E_0^{-\beta_+}\right) \times (1 - bEt)^{-2} \delta\left(E_0 - \frac{E}{1 - bEt}\right) dE_0, \tag{7}$$

where $r^2 = R^2 + z^2$. The integrations over E_0 and spatial coordinates are straightforward:

$$F_{e^+\rm ISM}(E) = \frac{c}{4\pi} \int_0^{1/bE} (\bar{n}_{\rm H} q_0 E^{-\beta_+}) \mathrm{erf}(Z_0/\sqrt{4\kappa t}) \times \exp(-t/\tau)(1 - bEt)^{\beta_+ - 2} dt \tag{8}$$

$$\approx \frac{c}{4\pi} (\bar{n}_{\rm H} q_0 E^{-\beta_+}) \int_0^{1/bE} \exp(-t/\tau)(1 - bEt)^{\beta_+ - 2} dt. \tag{9}$$

The approximation noted above is valid for small values of t, and yields the integral with an accuracy of ~10% or better. We have evaluated the integral in Equation (9) numerically. However, before we discuss this, it is useful to note that at very low energies, for $E \ll 1/b\tau$ we may set $(1 - bEt)^{\beta_+ - 2} \approx 1$ and $t_{\rm max} = \infty$, in Equation (9) and get

$$F_{e^+\rm ISM}(E) = \frac{q_0}{4\pi E^{\beta_+}} \bar{n}_{\rm H} c\tau \quad \text{for } E \ll 1/b\tau. \tag{10}$$

At very high energies $\tau \gg 1/bE$, (i.e., $\tau \gg t_{\rm max}$), we may set $\exp(-t/\tau) \approx 1$ in Equation (9) and evaluate the integral to get

$$F_{e^+\rm ISM}(E) = \frac{q_0 \bar{n}_{\rm H} c}{4\pi b(\beta_+ - 1)} \frac{1}{E^{\beta_+ + 1}}, \quad \text{for } E \gg 1/b\tau. \tag{11}$$

This is similar to earlier results (Cowsik et al. 1966). Now, to account approximately for solar modulation, which affect only the very lowest end of their spectrum, we get

$$F_{e+}(E) = F_{e+\rm ISM}(E) e^{-E_m/E} \tag{12}$$

and display this spectrum in Figure 1 for $\bar{n}_{\rm H} = 0.5$ cm^{-3}, $\tau = 2$ Myr and $E_m = 0.5$ GeV, which provide a good fit to the data. The product $m_{\rm H} \bar{n}_{\rm H} c\tau$ corresponds to a grammage $\Lambda_{e+} \approx 1.7\,\mathrm{g\,cm}^{-2}$. In order to visually assess the importance of the energy losses and solar modulation, we have displayed in Figure 1 the product $(q_0 \bar{n}_{\rm H} c\tau/4\pi) E^{-\beta_+}$, representing the spectrum of the positrons when the effects of energy loss and

solar modulation are suppressed. Note that the energy losses have steepened the high energy part of the positron spectrum to $E^{-3.65}$ and have made the spectral intensity independent of the leakage lifetime, a result that can be shown to be true even if τ were to be dependent on energy. The calculated spectrum of secondary positrons, using Equation (9), fits the observations well, for $\tau \approx 2$ Myr and the mean interstellar density $\bar{n}_{\rm H} \approx 0.5\,{\rm cm}^{-3}$. In the lower panel, the positron fraction, $R_{e+}(E)$ is displayed and fits the observations, as expected, because the e^+ spectrum agrees well with the calculation.

What is the expected behavior of the positron fraction at higher energies? In the energy region up to ~2000 GeV, we have the observations of the total electronic component, and the ratio $R_{e+}(E) = F_{e+}(E)/F_T(E)$ is easily calculated. As shown in Equation (6), the sharp steepening of $F_T(E)$ beyond ~1000 GeV is attributed to the discrete nature of the cosmic-ray sources and the energy losses suffered by the electronic component in the finite amount of time needed for them to arrive at the Earth (Cowsik & Lee 1979; Cowsik & Burch 2010; Shaviv et al. 2009; Nishimura et al. 1997). Even though the primary electronic component cuts off, the secondary electrons and positrons that are produced in the interstellar medium that surrounds the Earth suffer only the aforementioned steepening and continue as $\sim E^{-3.65}$ at least up to 10^4 GeV. At these energies secondaries dominate the flux and their ratio will be controlled by their production characteristics. As there exists an excess of protons over neutrons (bound in nuclei) in the primary cosmic-rays and because inelastic diffraction in the forward direction dominates the secondary cosmic-ray flux, e^+ is favored over e^- in the production. The secondary e^- is about ~0.5 of the e^+ (MS), and we therefore expect the $R_{e+}(E) = e^+/(e^+ + e^-)$ to reach ~0.7 at $E \gg 10^3$ GeV.

3. DISCUSSION

What are the significant differences between the two models, one exemplified by MS and the other described here, both displayed in the lower panel of Figure 1, that they make such diverse predictions for the positron fraction? The motivations for the cosmic-ray modeling has been provided by the observations of the ratio of secondary nuclei like B to that of their parent nuclei like C and O. Once the cross section for spallation is known then the grammage essentially controls the observed ratio, when effects of spallation and energy losses are to be taken into account (Davis et al. 2000; Cowsik et al. 1967). The transport parameters κ, τ, etc., in the current models (MS; Davis et al. 2000) are specified in terms of the rigidity and velocity. These are converted to grammage and are shown in Figure 3 as a function of kinetic energy per nucleon, E, or just kinetic energy for positrons. These models predict essentially the same energy dependence at $E \gtrsim 1$ GeV, but differ significantly at lower energies. However, at ~3 GeV the grammage of positrons is ~14 g cm^{-2} and for carbon it is ~7 g cm^{-2} because the carbon nuclei have higher rigidity by a factor of A/Z and a lower velocity compared to the positrons. On the other hand, in the alternate model (Cowsik & Burch 2010) discussed here, all the particles, independent of their energies, are assumed to have the same grammage $\Lambda \sim 1.7$ g cm^{-2} *in the Galaxy*. This is also shown in Figure 3. The rest of the *energy-dependent* grammage left over at lower energies, needed to explain the *energy-dependent* part of the B/C ratio, is attributed to traversal of material in a cocoon-like region surrounding the sources (Cowsik & Burch 2010; Ackerman et al. 2011; Binns 2011), discussed in the introductory section of this paper.

The following points comparing and contrasting the two models are noteworthy:

1. The energy dependence of the residence time, $\tau \sim E^{-0.6}$ of current models (MS, LB) will steepen the production spectrum $S_{e+} \sim E^{-2.65}$ to yield a steady state spectrum $E^{-3.25}$. The spectrum of the total electronic component is observed to be $\sim E^{-2.2}$ for $E < 6$ GeV and $E^{-3.1}$ at higher energies. Accordingly the positron fraction R_{e^+} in the current models will fall as $\sim E^{-0.95}$ below 6 GeV and more gently as $\sim E^{-0.15}$ at higher energies.
2. When the positron residence time is normalized to yield the current models (MS, LB), $\Lambda_{e+}(1\,{\rm GeV} < E < 3\,{\rm GeV}) \approx 14\,{\rm g\,cm}^{-2}$ as expected by modeling the B/C ratio, then the positrons are *overproduced* by a large factor at these energies.
3. This situation is to be contrasted with our model discussed here. The close similarity of the spectrum of positrons $E_{e+}(E) \sim E^{-2.65}$ and those of the parent primary cosmic-ray nuclei allows a good fit to the observations of $R_{e+}(E)$ up to ~300 GeV and predicts the smooth decrease at higher energies due to radiative losses suffered by the positrons. At very high energies beyond 1 TeV, the positron fraction increases again reaching an asymptotic value of ~0.7 when the primary electrons are cut off and only the secondaries are left behind.
4. Overproduction of positrons at low energies is avoided in the our model by the fact that the primary nuclei have 20–30 times higher energy than the positrons they produce, i.e., for positrons of a few GeV, the primary nuclei will be in the range $E \gtrsim 60\,{\rm GeV\,nucleon}^{-1}$ where the residence time in the sources is so short that the parent nuclei leak out without significant positron production (see Figures 2 and 3).
5. Finally, the ~2 Myr residence time in the Galaxy for all cosmic rays, at least up to several hundred TeV, allows one to predict the cosmic-ray anisotropies:

$$\frac{3\kappa}{c}\frac{\nabla n}{n} \approx \frac{3}{c}\frac{r^2}{4\tau}\frac{1}{r} \approx \frac{3r}{4c\tau} \approx 5 \times 10^{-4},$$

for the length scale $r \approx 500$ pc. This is consistent with an extensive compilation of the observations. As Strong et al. have noted in Figure 12 of their paper (Strong et al. 2007), the increase of the diffusion constant κ as $E^{0.6}$, which yields $\tau \sim E^{-0.6}$, concomitantly generates anisotropies that increase with increasing energy, significantly exceeding the observational bounds. This has led to considerable tension between upper bounds on anisotropy (Cowsik & Burch 2010) and those predicted by current models of cosmic ray propagation.
6. Radioactive nuclei in cosmic rays, such as ^{10}Be with a lifetime of ~2 Myr, offer opportunities for probing the characteristics of cosmic-ray propagation, especially at very low energies ~100 MeV nucleon^{-1}. The model presented here is consistent with the observations. A brief qualitative analysis is provided in the Appendix to this paper.

4. SUMMARY

In summary, the production of positrons by nuclear primary cosmic rays interacting with the interstellar medium provides a good explanation of the observed spectrum and fraction with respect to the total electronic component, provided these particles have an effective residence time of ~2 Myr in the

interstellar medium, independent of their energy. The prediction of the precise energy dependence of the positron fraction rests on a calculation of energy loss suffered by the positrons during their residence for ∼2 Myr in the interstellar medium, which leads to a spectrum $\sim E^{-3.65}$ for $E > 300$ GeV. The total electronic component has a spectrum $\sim E^{-3.1}$ up to ∼1000 GeV and rapidly decreases in intensity at higher energies, so that the positron fraction tends to reach an asymptotic value dictated by its production characteristics as secondaries, ∼0.7 for $E \gg 1000$ GeV. Because the sources of primary cosmic-ray electrons are discrete, their spectrum shows a cut-off at an energy ∼1000 GeV that is dictated by the distance to the nearest source. The spectrum of primary electrons may be understood as the sum of the contributions from various discrete sources, with the nearest source dominating at the highest energies (Cowsik & Burch 2010; Cowsik & Lee 1979; Nishimura et al. 1997; see also Equation (6) of this paper).

We thank professors M. H. Israel and S. Nussinov who played a key role in shaping these comments.

APPENDIX

RADIOACTIVE NUCLEI AND THE ^{10}Be/^{9}Be RATIO IN COSMIC RAYS

The spatial and temporal discreteness of cosmic ray sources have important implications on the fluxes of radioactive nuclei in cosmic rays. In the context of the Nested Leaky-box (NLB) model, we will show below that the observed ^{10}Be/^{9}Be ratio in cosmic rays can be reproduced correctly. Our analysis below considers only the spatial discreteness of the sources and this is adequate to indicate the consistency of the model with the observations.

The measurements and the implications of the secondary radioactive nucleus ^{10}Be have been well described by Yanasak et al. (Yanasak 2001). These measurements were carried out by satellite-borne instruments *Ulysses*, *ISEE-3*, *Voyager*, CRIS, and Solar Isotope Spectrometer instruments and cover the energy region ∼40–140 MeV nucleon^{-1}. Such radioactive nuclei constitute important probes of the processes of cosmic-ray generation and propagation, as the ratio of their abundances with respect to their radioactively stable isotopes can be used to determine the lifetime of cosmic rays in terms of the lifetime for radioactive decays.

In order to apply the transport equation that we have developed in the context of addressing the cosmic-ray positron spectra, the following considerations relevant for the propagation of ^{10}Be.

1. $\tau(^{10}\mathrm{Be}) \approx 2 \times 10^6$ yr.
2. ^{9}Be is the stable isotope and is produced in spallation reactions with approximately the same cross-section as ^{10}Be.
3. The energy loss suffered by these nuclei during propagation is not due to Compton scattering but due to ionization of the medium.

$$\left(\frac{dE}{dx}\right)_{\mathrm{Be}} \sim \left(\frac{Z^2}{A}\right)\left(\frac{dE}{dx}\right)_p \sim 1.6\left(\frac{dE}{dx}\right)_p \sim 3.2\,\mathrm{MeV\ nucleon^{-1}\,(g\,cm^{-2})^{-1}} \quad \text{(A1)}$$

at relativistic energies and increases at lower energies. We neglect this in the approximate discussion presented here.

4. The average velocity of Be nuclei over the range of observed energies ∼40 MeV nucleon^{-1} to 140 MeV nucleon^{-1} is ∼0.4 c. Because of this, we need to make the following changes:
   (a) The diffusion constant
   $$\kappa = \frac{1}{3} v\lambda \quad \text{(A2)}$$
   decreases with respect to the value at relativistic energies by a factor of v/c, even when one assumes that λ does not change.
   $$\kappa_{\mathrm{Be}} \lesssim (v/c) \times 10^{28}\,\mathrm{cm^2\,s^{-1}}.$$
   Keeping in mind a likely decrease in λ at very low energies, we assume $\approx 2\times10^{27}$ for illustrative purposes.
   (b) The escape lifetime, τ, is lengthened by at least a factor of c/v
   $$\tau_{\mathrm{Be}} \sim \tau_{e^+} c/v \sim 5\,\mathrm{Myr}.$$
5. We need to include the effect of the radioactive decay while addressing ^{10}Be and not while addressing ^{9}Be.
6. We neglect spallation of Be nuclei during propagation.
7. We also neglect the decay of ^{10}Be nuclei during the small amount of time they spend in the cocoon surrounding the sources.

With these considerations the transport equation (Equation (3)) now reads

$$\frac{\partial F_{10}}{\partial t} - \nabla\cdot(\kappa\ \nabla\ F_{10}) - F_{10}\left(\frac{1}{\tau_l}+\frac{1}{\tau_r}\right) = Q_{10}$$
$$\frac{\partial F_{9}}{\partial t} - \nabla\cdot(\kappa\ \nabla\ F_{9}) - F_{9}\left(\frac{1}{\tau_l}\right) = Q_{9}. \quad \text{(A3)}$$

The following notational changes have been made in presenting the analysis:
(a) $\kappa(^{10}\mathrm{Be}, ^{9}\mathrm{Be})$ is written at just K.
(b) The leakage lifetime, τ_{Be}, at ∼100 MeV nucleon^{-1} is written as τ_l.
(c) τ_r is the radioactive lifetime of ^{10}Be and appears only in the equation for F_{10}, the decaying isotope.

These two equations admit the following Green's functions:

$$G_{10} = (4\pi Kt)^{-3/2}\exp\left(-\frac{r^2}{4Kt} - \left[\frac{1}{\tau_l}+\frac{1}{\tau_r}\right]t\right)$$
$$G_{9} = (4\pi Kt)^{-3/2}\exp\left(-\frac{r^2}{4Kt} - \left[\frac{1}{\tau_l}\right]t\right). \quad \text{(A4)}$$

Now there are two components of Be nuclei in the observed flux of cosmic rays, first, the component generated by the spallation in the sources, and second, that generated by spallation in the general interstellar medium. The fluxes generated by a source located at r_s is given by

$$F_{10}(r_s) = \int_0^\infty (4\pi Kt)^{-3/2}\exp\left(-\frac{r_s^2}{4Kt} - \left[\frac{1}{\tau_l}+\frac{1}{\tau_r}\right]t\right)dt$$
$$F_{9}(r_s) = \int_0^\infty (4\pi Kt)^{-3/2}\exp\left(-\frac{r_s^2}{4Kt} - \left[\frac{1}{\tau_l}\right]t\right)dt. \quad \text{(A5)}$$

These integrals are evaluated numerically; they may be adequately approximated by

$$F_{10}(r_s) \sim \frac{\tau_l \tau_r}{\tau_l + \tau_r} \exp\left(-\frac{r_s^2}{6K}\left[\frac{1}{\tau_l} + \frac{1}{\tau_r}\right]\right)$$

$$F_9(r_s) \sim \tau_l \exp\left(-\frac{r_s^2}{6K}\left[\frac{1}{\tau_l}\right]\right). \quad \text{(A6)}$$

The ratio due to a source at r_s is given by

$$\frac{F_{10}(r_s)}{F_9(r_s)} \sim \frac{\tau_r}{\tau_l + \tau_r} \exp\left(-\frac{r_s^2}{6K\tau_r}\right) = 0.044. \quad \text{(A7)}$$

The value 0.044 is based on the choice $r_s = 1.7 \times 10^{21}$ cm and $\tau_l \approx 1.5 \times 10^{14}$ s, along with the well-established radioactive lifetime of ^{10}Be, $\tau_r = 6 \times 10^{13}$ s. Note that we need to sum F_{10} and F_9 over the set of sources in the Galaxy and that sources located farther away will lead to smaller ratios. We have used $r_s = 1.7 \times 10^{21}$ cm as an effective average. The numerical evaluation of Equation (A5) has been used to quote the value $F_{10}(r_s)/F_9(r_s) = 0.044$.

The second components of ^{10}Be and ^{9}Be arise through spallation in the interstellar medium. These fluxes are written compactly as

$$f_{10,g} \sim \iiint F_{10}(r) d^3\boldsymbol{r}$$

$$f_{9,g} \sim \iiint F_9(r) d^3\boldsymbol{r} \quad \text{(A8)}$$

(similar to Equations (7) and (8)). These are evaluated numerically. An analytical approximation yields similar values:

$$\frac{f_{10,g}}{f_{9,g}} \approx \frac{\tau_r}{\tau_l + \tau_r} \approx 0.29. \quad \text{(A9)}$$

The observations of the B/C ratios in cosmic rays in the energy region $E \lesssim 1$ GeV nucleon^{-1} indicate a 25% admixture of the contribution from the interstellar medium and 75% contribution from the sources in the NLB model. A corresponding admixture for the Be nuclei will lead to ratios similar to the observed value $\sim 0.11 \pm 0.02$:

$$R_{10,9} = (0.044 \times 0.75) + (0.29 \times 0.25) = 0.105.$$

There exists adequate latitude in the parameters like K and τ_l to fit the exact ^{10}Be/^{9}Be ratios when they are available. It is appropriate to recall here that Yanasak et al. (2001), in their analysis of the ^{10}Be/^{9}Be ratio in the context of the LB model, require a τ_l of $\sim$15 Myr to fit the observed ratio at $\sim$100 MeV nucleon^{-1}. The key difference in the NLB model is that the finite time needed for the propagation from the sources allows for the decay of the ^{10}Be component, significantly reducing its flux, and allows one to fit the observed ratios with a smaller residence time as described in this appendix.

REFERENCES

Ackerman, M., Ajello, M., Allafort, A., et al. 2011, Sci, 334, 1103
Ackerman, M., Ajello, M., Allafort, A., et al. 2012a, PhRvL, 108, 011103
Ackerman, M., Ajello, M., Atwood, W. B., et al. 2012b, ApJ, 761, 91
Adriani, O., Barbarino, G. C., Bazilevskaya, G. A., et al. 2009, Natur, 458, 607
Adriani, O., Barbarino, G. C., Bazilevskaya, G. A., et al. 2010, PhRvL, 105, 121101
Aguilar, M., Alberti, G., Alpat, B., et al. 2013, PhRvL, 110, 141102
Bergström, L., Bringmann, T., Cholis, I., Hooper, D., & Weniger, C. 2013, PhRvL, 111, 171101
Bergström, L., Edsjo, J., & Zaharijas, G. 2009, PhRvL, 103, 031103
Bernard, G., Arguin, J.-F., Barnett, R. M., et al. 2012, PhRvD, 86, 010001
Binns, W. R. 2011, Sci, 334, 1071
Blasi, P. 2009, PhRvL, 103, 051104
Chevalier, R. A., & Fransson, C. 2003, in Supernova Interaction with a Circumstellar Medium, ed. K. W. Weiler (Lecture Notes in Physics, Vol. 598; Berlin: Springer), 171
Cholis, I., & Hooper, D. 2014, PhRvD, 89, 043013
Cowsik, R. 1980, ApJ, 241, 1195
Cowsik, R., & Burch, B. 2010, PhRvD, 82, 023009
Cowsik, R., & Lee, M. A. 1979, ApJ, 228, 297
Cowsik, R., Pal, Y., Tandon, S. N., & Verma, R. P. 1966, PhRvL, 17, 1298
Cowsik, R., Pal, Y., Tandon, S. N., & Verma, R. P. 1967, PhRv, 158, 1238
Cox, A. N. 1999, Allen's Astrophysical Quantities (4th ed.; Melville, NY: AIP), 523
Davis, A. J., Mewaldt, R. A., Binns, W. R., et al. 2000, in AIP Conf. Proc. 528, Acceleration and Transport of Energetic Particles Observed in the Heliosphere, ed. R. A. Mewaldt et al. (Melville, NY: AIP), 421
Gaggero, D., Maccione, L., Di Bernardo, G., Evoli, C., & Grasso, D. 2013, PhRvL, 111, 021102
Jauch, J. M., & Rohrlich, F. 1996, The Theory of Photons and Electrons (2nd ed.; New York: Springer), 232
Katz, B., Blum, K., Morag, J., & Waxman, E. 2010, MNRAS, 405, 1458
Moskalenko, L., & Strong, A. 1998, ApJ, 493, 693
Mertsch, P., & Sarkar, S. 2009, PhRvL, 103, 081104
Nishimura, J., Kobayashi, T., Komori, Y., & Yoshida, K. 1997, AdSpR, 19, 767
Potgieter, M. S. 2013, LRSP, 10, 2
Profumo, S. 2012, CEJPh, 10, 1
Shaviv, N., Nakar, E., & Piran, T. 2009, PhRvL, 103, 111302
Strong, A., Moskalenko, I. V., & Ptuskin, V. S. 2007, ARNPS, 57, 285
Syrovat-skii, S. I. 1959, SvA, 3, 22
Telezhinsky, I., Dwarkadas, V. V., & Pohl, M. 2012, A&A, 541, A153
Witt, A. N., & Johnson, M. W. 1973, ApJ, 181, 363
Yanasak, N. F., Wiedenbeck, M. E., Mewaldt, R. A., et al. 2001, ApJ, 563, 768
Yuksel, H., Kirstler, M. D., & Stanev, T. 2012, PhRvL, 103, 051101